

Early recovery of Comet 55P/Tempel-Tuttle^{*}

O.R. Hainaut^{1,2}, K.J. Meech¹, H. Boehnhardt², and R.M. West³

¹ Institute for Astronomy, 2680 Woodlawn Drive, Honolulu, Hawaii 96822, USA

² European Southern Observatory, Casilla 19001, Santiago, Chile

³ European Southern Observatory, Karl-Schwarzschild-Strasse 2, D-85748 Garching bei München, Germany

Received 14 October 1997 / Accepted 5 January 1998

Abstract. We present recovery observations of the parent of the Leonid meteor stream – comet 55P/Tempel-Tuttle using the Keck II telescope. At recovery, the comet was at $r = 4.5$ AU, with $m_R = 22.6$, and there was no indication of coma or activity. Pre- and post-recovery observations from 6 observing runs (1994–1997 June) are presented. From these measurements we estimate that the nucleus radius is $R_N = 1.8 \pm 0.2$ km with a nucleus axis ratio greater than 1.5. As of 6/97 ($r = 3.5$ AU), the comet activity had not yet started.

Key words: astrometry – comets: individual: 55P/Tempel-Tuttle – meteors, meteoroids

1. Introduction

Comet 55P/Tempel-Tuttle, discovered independently on 19 December 1865 and 5 January 1866, is the parent of the Leonid meteor stream. The comet's revolution period is 33.23 years, and its next passage through perihelion will be on 1998 Feb. 28.10. Much more information is known about that stream than about its parent body; the Leonid stream has produced some of the greatest meteor storms in history, most notably that of 1833, with meteor rates up to $100\,000 \text{ hr}^{-1}$ (Kresák, 1993), and 1966, with rates up to $150\,000 \text{ hr}^{-1}$ (Milon, 1967). In fact, the Leonid showers have been documented back to 902 A.D. (Yeomans et al., 1996).

Unlike some comets where the dust evolution is dominated by ejection processes, radiation pressure and planetary perturbations play the major role in the case of 55P/Tempel-Tuttle. This has led to an uneven distribution of material in the orbit, where the material trails behind and outside the orbit of the comet. Leonid showers are most likely when the Earth trails the comet and passes just outside of the comet's descending node (Yeomans, 1981; Yeomans et al., 1996). Moreover, the dust is not spread along the orbit – possibly because of interaction with Uranus (Williams, 1997), therefore causing storms only during

a couple of years near the comet's perihelion passage. In non-storm years, the rate of meteors is relatively stable around $10\text{--}15 \text{ hr}^{-1}$. Based on an orbital analysis, Wu and Williams (1996) predict that the 1998/1999 Leonid storm will be unimpressive (e.g. average), however, Yeomans et al. (1996) suggest that there is the possibility of a significant display during both years. The 1997 shower was quite unimpressive, with rates peaking at $10\text{--}15$ meteors per hour (Hainaut, 1997).

Meteor streams provide an independent observation of comet dust from which we have inferred information on the physical nature of the dust, e.g. the chemical properties (spectroscopy) and density (Hajduk and Hajduková, 1990; McIntosh, 1991). The particles in the stream depend on the irregular mass loss from the parent, which in turn depends on the nucleus properties.

Comet 55P/Tempel-Tuttle is a Halley-family comet, *i.e.* it has migrated inwards from the Oort cloud via planetary perturbations. Unlike the observable short-period comets originating from the Kuiper belt, the Halley-family comets are probably less evolved than the Jupiter-family comets. Unfortunately virtually nothing is known about this comet: astrometric data are available from the 1699, 1865-66 and 1965 apparitions; from a 2000 year backward orbital integration Yeomans et al. (1996) believe that they may have identified observations of the comet by the Japanese in 1234 and the Chinese in 1035. Although the second comet spectrum ever taken was made of Tempel-Tuttle in 1866, no observations of the comet's physical behavior were made – even at the 1965 apparition, and thus no information is available about the dust and gas production.

The only observations of 55P/Tempel-Tuttle since its discovery in 1865 were during its 1965 apparition. The comet was recovered after an extensive orbital analysis (Schubart, 1965) but only 3 astrometric data points were obtained. In summary, virtually nothing is known about the parent of the Leonid stream. The comet will be making its closest approach to Earth in 132 years (Yeomans et al., 1996), passing within $\Delta = 0.36$ AU on 1998 January 17. This is the first apparition where modern detectors have been available to watch the development of the activity in the comet. The goal of the present program was to make an early observational recovery of the comet so that both nucleus observations and the development of the activity and measurement of the dust production could be made. In addition

Send offprint requests to: O.R. Hainaut, ESO-Chile

^{*} Based on observations collected at the European Southern Observatory, La Silla, Chile, and University of Hawaii and Keck observatories on Mauna Kea, Hawaii

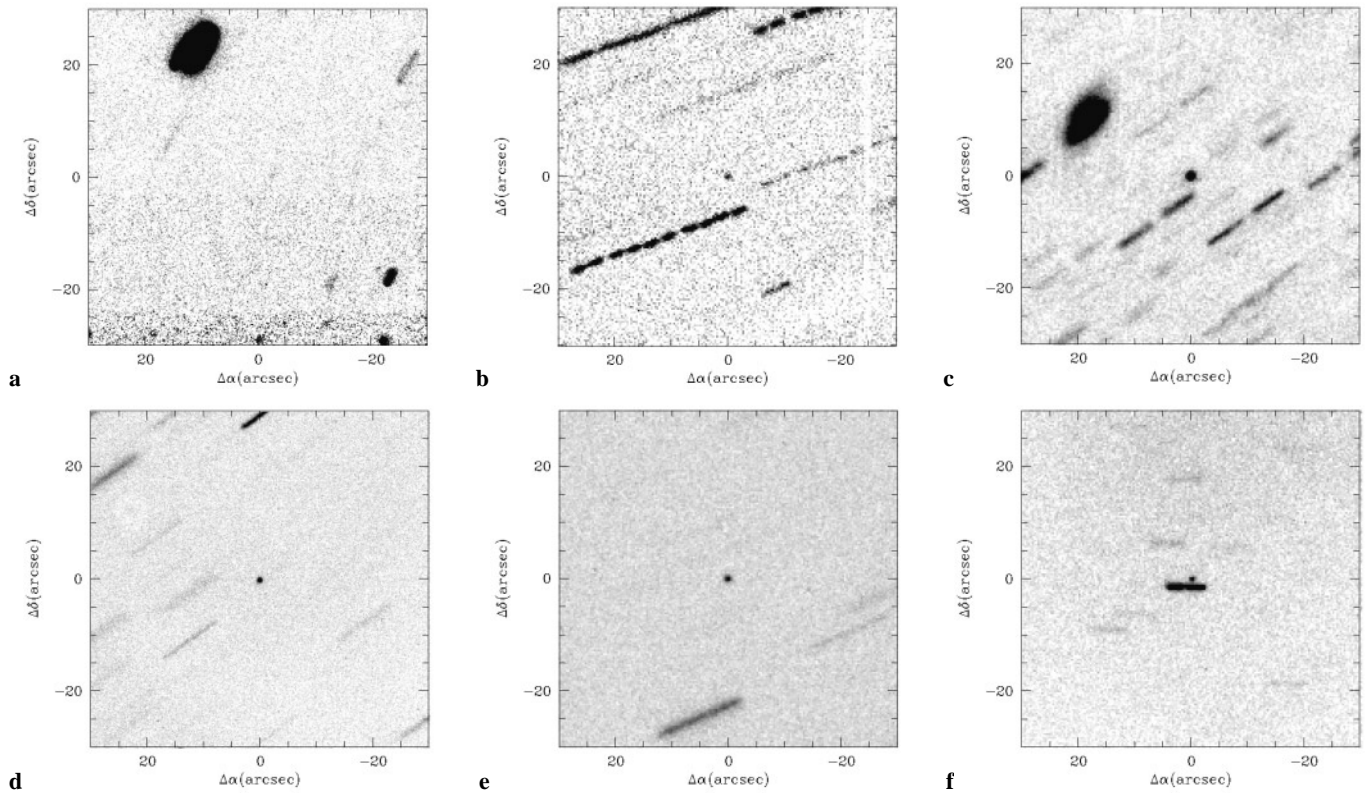


Fig. 1a–f Composite images of comet 55P/Tempel-Tuttle **a** 1995 Feb 04, **b** 1996 May 12, **c** 1997 Mar 04, **d** 1997 Mar 07, **e** 1997 Apr 17, and **f** 1997 Jun 17. North is up, East is left; all images have been obtained by co-adding all the frames obtained during that night after being shifted to compensate for the motion of the comet, whose expected position (using the post-recovery orbit) is at the center (0, 0) of the $60'' \times 60''$ frame sections shown.

to this program aimed at characterizing the nucleus, an extensive “International Leonids Watch” is planned for the 1998/1999 apparition; an increase in shower rates was first observed in 1994 and 1995 (Jenniskens, 1996).

2. Observations

During a program of very distant comet observations at the Keck II Telescope on 4 March 1997 we targeted 55P/Tempel-Tuttle for recovery (in part because the weather conditions were too poor for the main, very faint targets at $m_R \approx 28-29$). A moving object, most likely the comet, was easily visible in a 900 s integration. As this object did not display any evidence of coma or activity, it was not possible to identify it securely with Tempel-Tuttle on morphological grounds, since previously unknown asteroids in the field could not be ruled out a priori. Moreover, it is also not possible to unambiguously identify a comet by position and rate of motion alone without a second night of data to verify the orbit (Marsden, 1981; Marsden, 1994; Marsden, 1996a; Marsden, 1996b; Marsden, 1997; Bowell et al., 1989).

Since we had only obtained one night of data, insufficient for a safe recovery, we put out an urgent request for follow-up observations. Observations were made on 7 March 1997 using the ESO NTT telescope and the comet was subsequently reported as recovered (Hainaut et al., 1997; Martin et al., 1997).

Following the recovery observations, we analyzed data obtained prior to 1997, and were able to identify several pre-recovery images of the comet. Table 1 lists the circumstances of each of the observing runs; composite images of the comet are shown in Fig. 1.

2.1. 1994 May 10–11; $r = 10.8$ AU (NTT)

The images were obtained with the 3.54-m New Technology Telescope (NTT) at La Silla, on the Superb Seeing Imager (SuSI) installed at the $f/11$ Nasmyth-A focus, equipped with the CCD ESO#25, a Tektronix TEK 1024 Grade 1 (1024^2 pix) detector. The filter used was a Bessel V (ESO#641, $\lambda_0 = 5472\text{\AA}$, $\Delta\lambda = 1132\text{\AA}$ FWHM, peak transmission 80%). The $24\mu\text{m}$ pixels, covering $0''.128$ on the sky, were read binned 2×2 . The read-out noise was about $5.5e^-$ per binned pixel. The weather was perfect over the observatory, in spite of some worrisome cirrus over the Western horizon. The pre-recovery orbital elements used for these observations were unfortunately off by about $70''$ with respect to the position computed using the post-recovery elements, which is more than half the field-of-view of the SuSI camera ($2/2$). Thanks to the large offsets (up to $20''$) applied to the telescope for the image dithering, the actual position has been imaged on one of the individual frames. However, the limiting magnitude of that frame is only $m_R = 24.5$, which does

Table 1. Observing circumstances.

UT Date	Δ^1	r^1	Elong ²	Phase ³	Tel ⁴	Obs ⁵	Exp ⁶	Sky ⁷	Seeing ⁸	Pixel ⁹	Notes ¹⁰
1994 May 12	9.84	10.82	166.2	1.27	ESO NTT	OH	V _b 6000	21.4	1.10	0.128	1
1995 Feb 04	9.41	9.50	92.5	5.95	ESO NTT	RW	R _b 4000	21.0	0.71	0.128	
1996 May 12	5.85	6.74	149.5	4.37	ESO 2.2m	RW	R _b 5360	20.8	1.00	0.332	
1997 Mar 04	3.65	4.45	139.5	8.32	Keck II	KM,OH,JB	R _k 1800	20.5	0.82	0.219	2
1997 Mar 07	3.60	4.43	142.6	7.83	ESO NTT	PM	R _b 900	20.4	0.65	0.128	
1997 Apr 17	3.14	4.06	155.0	6.05	UH 2.2m	KM,OH,JB	R _k 2850	20.0	0.50	0.219	3
1997 Jun 17	3.48	3.48	81.7	16.79	UH 2.2m	OH,CD	R _k 1200	19.0	0.74	0.144	

Notes: ¹Geocentric and Heliocentric distances [AU] of observation – ²Solar elongation [deg] – ³Phase Angle [deg] of observations – ⁴Telescope: ESO NTT: 3.54m New Technology Telescope, European Southern Observatory, La Silla, Chile; ESO 2.2: 2.2m ESO/Max Planck Gesellschaft, ESO, La Silla, Chile; UH 2.2: 2.2m University of Hawai‘i, Mauna Kea; Hawai‘i; Keck II: 10m Keck-II, W.M. Keck Foundation, Mauna Kea, Hawai‘i; ⁵Observer: CD: Catherine Delahodde; HB: Hermann Boehnhardt; JB: James Bauer; KM: Karen Meech; OH: Olivier R. Hainaut; PM: Pierre Martin and the NTT Team; RW: Richard M. West – ⁶Filter and Exposure time [seconds]; V_b, R_b: Bessel system, R_k: Kron-Cousin R. – ⁷Sky brightness [mag arcsec⁻²] – ⁸Seeing [arcsec] – ⁹Pixel scale [arcsec] – ¹⁰ Comments: 1: CCD read binned 2 × 2 – 2: weather not photometric – 3: weather probably not photometric

not provide a very constraining limit to the size of a cometary nucleus at 10 AU.

2.2. 1995 February 3–4; $r = 9.5$ AU (NTT)

The instrumental set-up was the same as for the 1994 run (the CCD was read un-binned; read noise $\sim 5.9e^-$); the images were taken through the Bessel R filter ESO#642 ($\lambda_0 = 6433\text{\AA}$, $\Delta\lambda = 1667\text{\AA}$ FWHM, peak transmission 85%); the weather was perfect. As for the 1994 observations, the ephemerides computed using the pre-recovery elements were off by almost $60''$. Fortunately, the images obtained during the second night show the post-recovery-expected position for the comet close to the edge of the composite image. A 2.4σ object about $3''$ from the expected position is visible on the composite 4000 s image. It is too faint to be visible in the single frames, or even in partial composites. While the object is probably the comet, the 2.4σ level does not ensure a high enough statistical significance (the probability for the candidate to be a noise feature, or the probability to have a 2.4σ noise feature of about $1''$ diam. within $3''$ of the expected position, is about $(1 - 0.984) \times 3/1 \simeq 5\%$), therefore, we cannot consider it to be a secure detection. The 3σ limiting magnitude is reported as upper limit for the brightness in Table 3.

2.3. 1996 May 12; $r = 6.7$ AU (ESO/MPI 2.2-m)

The observations were performed on the ESO/MPI 2.2-m telescope at La Silla, using the EFOSC2 spectro-imager equipped with the CCD ESO#19, a front-side illuminated, UV coated Thomson 31156 Grade A detector (1024×1024 , $19\mu\text{m}$ pix), whose readout noise was $3.3e^-$ rms, and gain $2.0e^- \text{ADU}^{-1}$. The camera was operated at $f/4.9$, giving a $5.7 \times 5.7'$ field ($0''.332$ pix). The filter used was a Bessel R (ESO#585, $\lambda_0 = 6431\text{\AA}$, $\Delta\lambda = 1654\text{\AA}$ FWHM, peak transmission 86%). While the comet was not visible on most of the single frames (300 s exposure each, except for one of 270 s), it appeared on some of

them, and is clearly visible on a composite made from half of the available single frames. Because of its faintness, the comet was not immediately identified when the images were taken, and it was only after the recovery with the Keck telescope had led to an improved orbit that we were able to identify the comet on these pre-recovery frames.

2.4. 1997 March; $r = 4.5$ AU

March 4, Keck-II – Images were obtained with the LRIS imaging spectrometer from the remote observing room in Waimea. In the imaging mode, the plate scale is $0''.215 \text{pix}^{-1}$, with a useful area of 1660×2048 pixels. The gain of the detector is $1.97e^- \text{ADU}^{-1}$ with a readout noise of $6.3e^-$. Several hours during the first half of the night were lost because of a coolant leak from the instrument. After repairs, we were just coming on line again when thick clouds appeared. We quickly changed our program to look at brighter objects and targeted 55P/Tempel-Tuttle. We obtained 7 images of the comet – 4 of which were very bad because of clouds (very poor S/N, poor image quality). The 3 remaining ones were fortunately obtained through gaps between clouds and are the deepest of all the Tempel-Tuttle images reported here.

March 7, NTT – While the S/N of the March 4 images did not leave any doubt about the reality of the object, its stellar appearance and the short time span covered by the Keck observations left some doubt about the identity of the object. However, a few days later, a single, 900 s image was obtained under excellent seeing condition at the NTT by P. Martin and the NTT team, showing the object at the expected position (and motion) and thus confirming its identity. The image was obtained with the SuSI camera, equipped with CCD ESO#42, a back illuminated Tektronix TeK1024A ($24\mu\text{m}$ pix, readout noise $4.6e^-$), through a Bessel R filter (ESO#642). The frame was processed by the NTT team, and transferred electronically to Hawai‘i where the comet was measured (photometry and astrometry).

2.5. 1997 April 15,17; $r = 4.08$ AU (UH 2.2m)

Images were obtained on 1997 April 15 using the UH 2.2m telescope with the Tektronix 2048 CCD camera at the f/10 Cassegrain focus. The plate scale in this configuration is $0''.219 \text{ pix}^{-1}$, and the detector had a gain of $1.8e^- \text{ ADU}^{-1}$ and a readout noise of $\approx 25 e^-$. The night started with some high altitude clouds and high humidity, however by 8 UT the sky appeared clear, and the humidity had dropped enough to open by 10:30 UT. Although the night appeared photometric after opening, and some standards were taken, the 55P/Tempel-Tuttle fields were re-calibrated on the following night. Images were also obtained on 1997 April 17, also during non-photometric conditions.

2.6. 1997 June 18; $r = 3.5$ AU (UH 2.2m)

Director's discretionary time was obtained on the UH 2.2m from 1997 June 17-19 UT for the purpose of calibrating comet data taken on previous runs under non-photometric conditions. The same Tektronix 2048 CCD was used with the f/31 focus giving a plate scale of $0.14''$ per binned pixel and a $2.4'$ FOV. On the first night of the run all of the previous 55P/Tempel-Tuttle images were re-calibrated, and on 1997 June 18 additional images of the comet were obtained.

3. Data reduction

3.1. Image processing

Because of the very faint limiting magnitudes we want to reach for our distant comet observing programs, special care was taken to obtain very high quality ancillary calibration frames; the image processing techniques have also been carefully optimized for the minimization of the noise. All the image processing was performed using MIDAS ("Munich Image and Data Analysis System," an interactive package developed and maintained by ESO, which allows the user to write procedure in a special language, possibly calling some FORTRAN or C programs). A template bias frame was created by taking the 2-dimensional median of a collection of many zero second exposures obtained at the beginning and end of each night. This composite bias was subtracted frame by frame from all the raw data. Additional variations of the global bias level were corrected by using the mean of the overscan region of each frame. The dark current was estimated using long, dark exposures; in all cases, it was found small enough to be neglected. Special care was taken to generate excellent detector sensitivity maps, or flat-fields, that correct all the sensitivity variations without introducing any significant amount of noise. Ideally, for each night, a series of dome flat-fields and sky twilight flat-fields were obtained. They were bias subtracted, then normalized to a mean level of 1, and median averaged to form a template dome flat-field and a template twilight flat-field. The long scientific exposures are themselves very valuable as flat-fields, as the sky color and detector illumination are exactly those prevailing during the observations, while the twilight and especially the dome flats are obtained with

a different color of light and type of illumination. In order to use the science images as flat-fields, it is important to dither the telescope between each of the exposures, so that a given object always falls on a different part of the detector. Tables of random offsets are generated in advance for that purpose. The scientific images are normalized so that their mean sky level is equal to 1, the brightest stars and objects of each frames are marked, and all the frames are median averaged (rejecting the marked regions, if necessary), forming a template science flat-field.

Each of the three template flat-fields has its advantages and problems: the dome flat has an excellent signal-to-noise ratio, but very poorly represents the large scale variations of sensitivity; the twilight flat has also a good signal-to-noise ratio, and better represents the large scale variations of the flat-field. These variations are perfectly measured by the science frame flat, but this flat has a very poor signal-to-noise ratio (being the average of only a few frames, each one having only a few hundred to thousand counts), and is therefore useless for small scale sensitivity variations. If only one of the three templates can be used, the twilight flat is a very good compromise. When possible, however, full advantage of each of the templates can be utilized (Hainaut et al., 1994). To do this, we separated each of template flats into a series of frames, each containing the information from the sensitivity map for a range of spatial frequencies (pixel-to-pixel variations, small scale variations, small scale gradients to finally large scale gradients). This separation is performed using a wavelet decomposition package implemented in MIDAS. The final flat-field template is obtained by combining the frames corresponding to the frequencies that each of the templates sample the best. While the actual combination varies from situation to situation, a typical example would be

$$F_f = \frac{1}{2}(D_{\text{high_frq}} + T_{\text{high_frq}}) + T_{\text{med_frq}} + S_{\text{low_frq}}, \quad (1)$$

where F_f is the final flat field, D is the dome flat, T is the twilight flat, and S is the science flat.

3.2. Photometric calibration

The images presented in this paper were obtained over a long time period, using different detectors and telescopes; moreover, some of the observing runs were not photometric. Therefore, we preferred to re-calibrate all the data in order to achieve a better uniformity. During the June 1997 run, all the fields were re-imaged using the UH2.2m telescope, through the Kron-Cousins R and I filters (R: $\lambda_o = 6460\text{\AA}$, $\Delta\lambda = 1245\text{\AA}$; I: $\lambda_o = 8260\text{\AA}$, $\Delta\lambda = 1888\text{\AA}$). During this run, we also obtained images of a large number of photometric standard fields (Landolt, 1992) at a wide range of airmasses, ensuring a complete calibration of the system used, including the atmospheric extinction and the color terms of the photometric transformation. The magnitude of the comet (or the limiting magnitudes) during the other runs was determined from relative photometry using all the stars visible in the original and June 1997 images. The magnitude of the comet was obtained using a color $R-I = 0.35$ for the

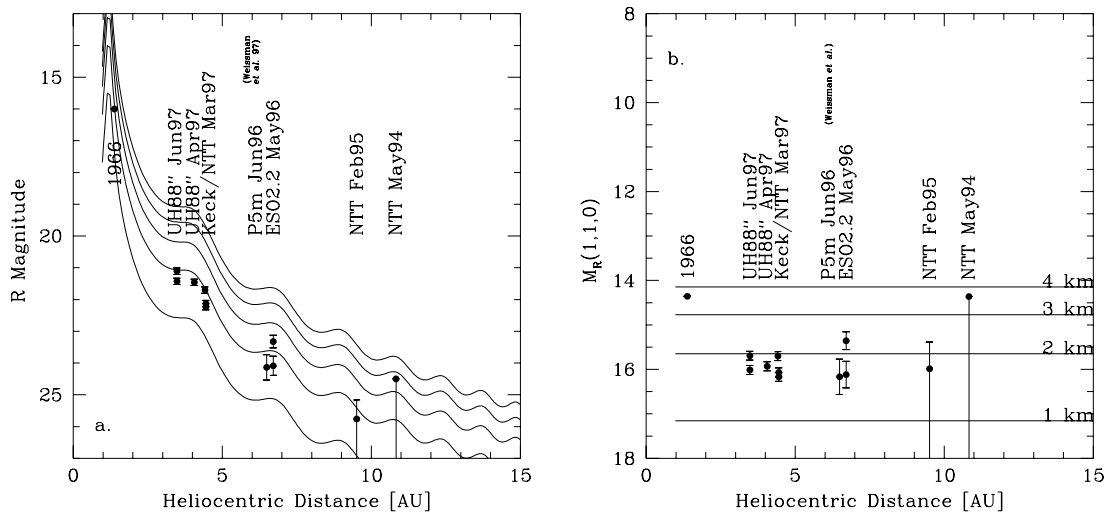


Fig. 2. **a** Lightcurve of 55P/Tempel-Tuttle (the photometric errors are indicated with bars) as a function of the heliocentric distance. Pre-recovery upper limits are shown for the 1994 and 1995 NTT data. The solid lines are the lightcurves of nuclei of different radii (1 to 5 km, 5 km is the upper curve). The undulations are caused by the annual variations in the geocentric distance of the comet. The measurements from Weissman and Buratti (1997) at Palomar and the 1966 apparition point (when the comet was active) are also plotted. Plot of $m_{1,1,0}$ as a function of r . The data are consistent with no activity from a 1.8 km radius nucleus.

Table 2. Comet 55P/Tempel-Tuttle astrometry

UT Date	$\alpha_{(J2000)}$	$\delta_{(J2000)}$	Obs.
1996 05 12.09294	13:38:41.72	+00:16:22.2	809
1996 05 12.13955	13:38:39.77	+00:16:33.2	809
1996 05 12.11580	13:38:40.79	+00:16:27.5	809
1997 03 04.62838	13:43:12.63	+04:43:37.7	568
1997 03 04.63700	13:43:12.31	+04:43:41.7	568
1997 03 04.64876	13:43:11.57	+04:43:49.0	568
1997 03 04.65752	13:43:11.07	+04:43:54.4	568
1997 03 07.31080	13:40:40.80	+05:10:45.3	809
1997 04 17.46832	12:45:38.17	+12:43:18.2	568
1997 06 18.30963	11:36:32.60	+17:21:54.0	568
1997 06 18.31785	11:36:32.37	+17:21:53.2	568

color transformation; this color was selected as the mean of a well measured sample of cometary nuclei (Meech, 1998). Note that the change introduced by the use of another value would be much smaller than the other errors.

3.3. Astrometric calibration

The position of the comet was calibrated using the position of field stars as measured on the Digital Sky Survey. At least 5 or 6 stars were used in the transformations; the RMS residuals of the transformation are 0.1–0.4'' depending on several factors, including the number and brightness of the stars, and their trailing in the original images. All the frames were registered with respect to each other using several stars visible in each image. The registered frames were then calibrated astrometrically, and the expected position of the comet was obtained using its equatorial position computed for the epoch of the mid-exposure and the astrometric transformation. The frames were also co-added

after registration on the expected position of the comet. The resulting composites show the stars as long trails, and the comet (whenever visible) as a point source. It should be noted that the trails are not necessarily straight lines, since the ephemerides used for the dithering took into account the variations of the comet's proper motion caused by the earth's rotation (daily parallax). The astrometry for 55P/Tempel-Tuttle is shown in Table 2, with the observatory code indicated (568=Mauna Kea; 809=La Silla).

4. Discussion

4.1. Absolute magnitude and nuclear diameter

Assuming that the comet does not display any cometary activity, its brightness should strictly follow an inverse square law which can be expressed as:

$$m_{r,\Delta,\alpha} = m_{1,1,0} + 5 \log(r\Delta) + 0.04 \alpha, \quad (2)$$

where $m_{1,1,0}$ is the magnitude normalized to $r = \Delta = 1$ AU and the phase angle $\alpha = 0^\circ$. The 0.04α term is an empirically determined correction of the phase effect (Meech and Jewitt, 1987). This relation may of course be modulated by brightness variations due to the unknown rotation of the comet. In Table 3 we present the photometry for all of the runs (average m_R magnitudes), and in addition have presented the $m_{1,1,0}$ values calculated from the data. The photometry was measured in a very small aperture (typically $2\times$ the seeing) in order to minimize the sky noise contribution to the measurement. The data do not show any systematic deviation from an inverse square law, thus we interpret this to mean that the comet was not active, even at $r = 3.5$ AU. The m_R magnitude reduced to $\Delta = r$ is plotted in Fig. 2a, and Fig. 2b shows the $m_{1,1,0}$ magnitude. A photometric measurement of 55P/Tempel-Tuttle was obtained by Weissman

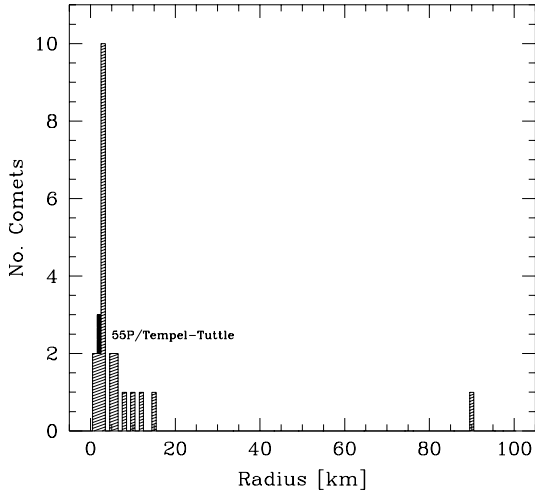


Fig. 3. Comparison of nucleus sizes for 24 nuclei – after Meech (1998); 55P/Tempel-Tuttle is highlighted.

and Buratti (1997) at the Palomar 200'' telescope on June 16, 1996, while the comet was at $r = 6.49$ AU. The magnitude $m_R = 24.5$ is compatible with our results. This data point has been plotted together with ours for comparison.

The weighted mean value of $m_{1,1,0}$ may be used to compute the radius, R_N , of 55P/Tempel-Tuttle (Russell, 1916):

$$p_v R_N^2 = 2.235 \times 10^{22} r^2 \Delta^2 10^{0.4(m_\odot - m_R)}. \quad (3)$$

where $p_v = 0.04$ is assumed for the geometric albedo and $m_\odot = -27.10$ is the red solar magnitude. The radii derived from this equation are shown in Table 3. Although these values correspond to a small nucleus, they are consistent with what is being found for other comet nuclei (Meech, 1998). The average value of the nucleus radius is

$$R_N = 1.78 \pm 0.23_{\text{statistic}} \pm 0.08_{\text{photometric(average)}} \text{ km}. \quad (4)$$

A comparison of the sizes of cometary nuclei measured so far is shown in Fig. 3.

The amplitude of any observed lightcurve caused by rotation of the nucleus may be used to obtain a minimum axis ratio for the comet. None of the runs have sufficient time base coverage to constrain the rotation; however, on several runs (1996 May, 1997 March and 1997 June) more than 1 image was taken, and in all cases the difference between the magnitudes obtained from the images was greater than the errors (*i.e.* significant). In order to estimate the axis ratio, we make the assumption that these differences are entirely caused by the rotation, and not at all by the photometric errors, nor by possible albedo variations. We also assume that the bare nucleus can be modeled as a tri-axial ellipsoid with axis dimensions $a > b > c$. If the comet is rotating along the shortest axis, then the area of the nucleus projected on the plane of the sky would vary from πac to πbc (if the aspect angle is 90° ; or πab for an aspect angle of 0°). The measured lower limit to the amplitude of the lightcurve can then be interpreted as a lower limit

$$\epsilon = b : a \leq 10^{-0.4\Delta m}, \quad (5)$$

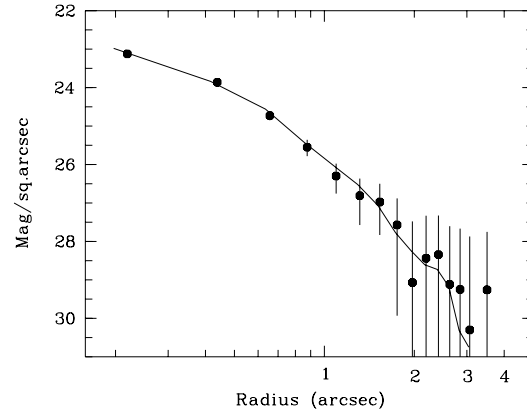


Fig. 4. Radial surface brightness profile of 55P/Tempel-Tuttle (filled circles) compared to a stellar profile from the 1997 March 4 Keck run.

Table 3. Comet 55P/Tempel-Tuttle photometry

UT Date	r [AU]	m_R	$m(1,1,0)$	R_N [km]
1994 May 12	10.8	>24.5	>14.31	<4.7
1995 Feb 4	9.5	$\gtrsim 25.7$	$\gtrsim 15.74$	$\lesssim 1.9$
1996 May 12	6.7	23.9-24.2	15.36-16.12	1.6-2.3
1997 Mar 04	4.5	22.6	16.07-16.17	1.6
1997 Mar 07	4.5	22.3	15.70	1.9
1997 Apr 17	4.1	21.7	15.92	1.9
1997 Jun 17	3.5	21.7-22.1	15.61-16.01	1.7-2.0

where Δm is the full range of the lightcurve in magnitudes. Using this equation, we obtain a lower limit to the axis ratio for the comet of $\epsilon = 1.5$, corresponding to the largest change in brightness, which occurred during the 1996 May run.

4.2. Cometary activity

Although observations of deviations from the inverse square law on the heliocentric lightcurve is the most sensitive way to detect any cometary activity (this was the method by which activity was first detected on comet 1P/Halley; Meech et al. (1986)) we have computed the radial surface brightness profile of the comet compared to field stars to see if there is any evidence of image extension indicative of a coma. This is done by computing the sky subtracted total counts in concentric annuli centered on the peak pixel and using the photometric transformations to place this on an absolute scale. As shown in Fig. 4, the profile is consistent with a bare nucleus.

4.3. Future plans

We intend to continue to observe this comet as often as possible in order to study the onset of the dust production and also to monitor the further development. During the fall of 1997, in collaboration with M. A'Hearn and Y. Fernandez, we will be observing the comet simultaneously in the optical and IR from

Mauna Kea, in an attempt to directly measure the nucleus size and albedo.

5. Conclusions

We have recovered the periodic comet 55P/Tempel-Tuttle using the Keck 10-m telescope on 07 March 1997 when the comet was at a distance of $r = 4.43$ AU; the observation was confirmed 3 nights later by means of observations with the ESO NTT. At the time of recovery, the comet was not active. From a new orbital solution, based on previous apparitions and on the recovery image, we were able to identify pre-recovery images of the comet at $r = 6.74$ AU, and upper limits to the brightness on 2 additional dates. By the time of our last observation, at 3.48 AU, the comet was still inactive. From the average $m(1,1,0)$ found from the data ($m_{1,1,0} = 15.9 \pm 0.1$), we have determined that the rotationally averaged nucleus radius to be $R_N = 1.8 \pm 0.2$ km, with a minimum ellipticity $b : a = 1.5$.

Acknowledgements. We would like to thank James Bauer for his help with the 1997 March Keck observations, and Catherine Delahodde for help with the 1997 June observations and the data reduction. We would especially like to thank the ESO team (P. Martin, K. Mueller, G. Van de Steene, N. Hurtado and J. Miranda) for being able to reschedule part of their night to obtain the followup recovery observation on 1997 March 7, with a noteworthy rapidity and efficiency, and Paul Weissman for making his data available to us. In addition, we thank Brian Marsden for updating the orbits so we could recover the comet. The Digital Sky Survey was produced at the Space Telescope Science Institute under U.S. Government grant NAG W-2166 (for a complete list of contributions to the DSS, please refer to http://stdata.stsci.edu/dss/dss_acknowledgements.html). Support for this work was provided by NASA Grant No. NAGW 5015, and an NSF REU Supplement to Grant No. AST 92-21318.

References

- Bowell, E., Chernykh, N. W., and Marsden, B. G.: 1989, Asteroids R. P. Binzel, T. Gehrels and M. S. Matthews (Eds), Chapt. Discovery and Follow up of Asteroids, pp 21–38, Univ. AZ Press
- Hainaut, O. R.: 1997, Visual observations of the 1997 Leonid Meteors, Priv. Communication
- Hainaut, O. R., Meech, K. J., and Bauer, J. M.: 1997, IAU Circ. 6579
- Hainaut, O. R., West, R. M., Smette, A., and Marsden, B. G.: 1994, A&A **289**, 311
- Hajduk, A. and Hajduková, M.: 1990, in Asteroids, Comets, Meteors III, C.-I. Lagerkvist et. al. (Eds), pp 531–534, Uppsala Univ.
- Jenniskens, P.: 1996, Meteoritics & Planetary Sciences **31**, 177
- Kresák, L.: 1993, Meteoroids and Their Parent Bodies, J. Stohl, I. P. Williams (Eds.), p. 147, Ast. Inst of the Slovak Academy of Sciences, Slovakia
- Landolt, A.: 1992, Astrophys. J. **104**, 340
- Marsden, B. G.: 1981, IAU Circ. 3619
- Marsden, B. G.: 1994, Minor Planet Circ. 23697
- Marsden, B. G.: 1996a, Minor Planet Circ. 28335
- Marsden, B. G.: 1996b, in IAU Symp. 172, Ferraz-Mello and Morando and Arlot (Eds.), pp 153–164, Kluwer
- Marsden, B. G.: 1997, Minor Planet Circ. 30117
- Martin, P., Mueller, K., van de Steene, G., Hurtade, N., and Miranda, J.: 1997, IAU Circ. 6579
- McIntosh, B. A.: 1991, Comets in the Post-Halley Era, R. L. Newburn and et al. (Eds.), Chapt. Debris from Comets: The Evolution of Meteor Streams, pp 557–591, Kluwer, Dordrecht
- Meech, K. J.: 1998, in Asteroids, Comets, Meteors 1996, in press
- Meech, K. J. and Jewitt, D. C.: 1987, A&A **187**, 585
- Meech, K. J., Jewitt, D. C., and Ricker, G. R.: 1986, Icarus **66**, 561
- Milon, D.: 1967, J. Br. Astron. Assoc. **77**, 89
- Russell, H. N.: 1916, ApJ **43**, 173
- Schubart, J.: 1965, IAU Circ. 1907
- Weissmann, P. R. and Buratti, B.: 1997, Observations of Comet Tempel-Tuttle with the Palomar 200inch Telescope, private communication
- Williams, I. P.: 1997, in XXIIIrd General Assembly of the International Astronomical Union, Kyoto August 17-30, 1997
- Wu, Z. and Williams, I. P.: 1996, Mon. Not. R. Astron. Soc. **280**, 1210
- Yeomans, D. K.: 1981, Icarus **47**, 492
- Yeomans, D. K., Yau, K. K., and Weissman, P. R.: 1996, Icarus **124**, 407